THE JOURNAL OF BIOLOGICAL CHEMISTRY
Vol. 276, No. 12, Issue of March 23, pp. 9246–9252, 2001

Printed in U.S.A.

Structure of a Multifunctional Protein

MAMMALIAN PHOSPHATIDYLINOSITOL TRANSFER PROTEIN COMPLEXED WITH PHOSPHATIDYLCHOLINE*

Received for publication, November 7, 2000, and in revised form, November 27, 2000
Published, JBC Papers in Press, December 4, 2000, DOI 10.1074/jbc.M010131200

Marilyn D. Yoder‡§, Leonard M. Thomas‡¶, Jacqueline M. Tremblay‖, Randall L. Oliver‡, Lynwood R. Yarbrough‖‡‡, and George M. Helmkamp, Jr.‖‡‡**

From the ‡Division of Cell Biology and Biophysics, School of Biological Sciences, University of Missouri-Kansas City, Kansas City, Missouri 64110-2499 and the ‖Department of Biochemistry and Molecular Biology, University of Kansas Medical Center, Kansas City, Kansas 66160-7421

Eukaryotic phosphatidylinositol transfer protein is a ubiquitous multifunctional protein that transports phospholipids between membrane surfaces and participates in cellular phospholipid metabolism during signal transduction and vesicular trafficking. The three-dimensional structure of the α-isoform of rat phosphatidylinositol transfer protein complexed with one molecule of phosphatidylcholine, one of its physiological ligands, has been determined to 2.2 Å resolution by x-ray diffraction techniques. A single β-sheet and several long α-helices define an enclosed internal cavity in which a single molecule of the phospholipid is accommodated with its polar head group in the center of the protein and fatty acyl chains projected toward the surface. Other structural features suggest mechanisms by which cytosolic phosphatidylinositol transfer protein interacts with membranes for lipid exchange and associates with a variety of lipid and protein kinases.

Phosphatidylinositol transfer proteins (PITPs)[1] constitute a highly conserved family of proteins in multicellular animals, with members in species ranging from *Homo sapiens* to *Dictyostelium discoideum* (reviewed in Refs. 1–2, see also Refs. 3–5). PITPs catalyze an exchange of phosphatidylinositol (PtdIns) or phosphatidylcholine (PtdCho) molecules between the surfaces of biological or artificial membranes. The protein appears to be multifunctional, with cellular functions ranging from intermembrane phospholipid transport to possible substrate presentation to lipid-modifying enzymes. Exogenous PITP is able to restore hormone-stimulated G protein-coupled activation of PtdIns(4,5)P_2 hydrolysis in human promyelocytic cells (6) and to reconstitute Ca^{2+}-stimulated, ATP-dependent secretion of catecholamines in rat pheochromocytoma cells (7). A variety of cultured mammalian cells respond to peptide agonists, epidermal growth factor, and antigens for the IgE receptor with a PITP-dependent stimulation of PtdIns 4-kinase and phospholipase C (8–9). PITP and PtdIns 3-kinase together exhibit a capacity to phosphorylate PtdIns to PtdIns(3)P (10). In cell-free systems the budding of vesicles from the *trans*-Golgi network and vesicle transport between *cis* and *medial* Golgi compartments are both stimulated by PITP (11–12). Existence of PITP-containing multiprotein complexes has been proposed, poised to respond to extracellular stimuli and to channel PtdIns efficiently from PITP to kinases and phospholipases for the generation of signal transducing molecules and regulation of vesicular trafficking (13–14).

Multiple isoforms of cytosolic, 32-kDa PITPs are common and ubiquitous (15–16). Mammalian PITPα and PITPβ share nearly 80% sequence identity; both isoforms are capable of forming noncovalent and stoichiometric complexes with PtdIns or PtdCho and transporting these lipid substrates through an aqueous environment. Sequence identity is more than 98% among mammalian PITPα isoforms (Fig. 1). PITPα and PITPβ represent unique gene products (17p13.3 and 22q12.1, respectively, in humans) and they exhibit differential tissue expression. The N terminus of the 140-kDa membrane-associated retinal degeneration B proteins (rdgBs) contains a region homologous to the soluble PITPs (17–20). Significantly, the rdgB-PITP region, comprising 266 amino acids, can be expressed as a soluble protein that exhibits both PtdIns and PtdCho transfer activities. We have solved the structure of rat PITPα bound to phosphatidylcholine using x-ray diffraction techniques. The results provide a framework for understanding the interactions of PITPs with lipid molecules and membrane surfaces in lipid transport processes and with other cellular proteins during signaling and trafficking events.

EXPERIMENTAL PROCEDURES

Protein Preparation and Crystallization—There were two criteria that guided all crystallization experiments: use of unmodified protein and maintenance of a protein-bound ligand of physiological significance. Considerable biochemical data have accumulated indicating that the C-terminal residues of PITP exhibit a conformational change upon binding to membranes. We therefore avoided the use of truncated or

* This work was supported by National Institutes of Health Grants GM24035 (to G. M. H. and L. R. Y.) and GM59162 (to G. M. H., L. R. Y., and M. D. Y.), the American Heart Association (to L. R. Y.), and the University of Kansas Medical Center Research Institute (to G. M. H.). The costs of publication of this article were defrayed in part by the payment of page charges. This article must therefore be hereby marked "*advertisement*" in accordance with 18 U.S.C. Section 1734 solely to indicate this fact.

The atomic coordinates and structure factors (code 1FVZ) have been deposited in the Protein Data Bank, Research Collaboratory for Structural Bioinformatics, Rutgers University, New Brunswick, NJ (http://www.rcsb.org/).

§ To whom correspondence should be addressed: Division of Cell Biology and Biophysics, School of Biological Sciences, University of Missouri-Kansas City, 5100 Rockhill Rd., Kansas City, MO 64110-2499. Tel.: 816-235-1986; Fax: 816-235-1503; E-mail: yoderm@umkc.edu.

¶ Present address: Howard Hughes Medical Inst., Division of Biology, California Inst. of Technology, Pasadena, CA 91125.

** Present address: Zymogenetics, 1201 Eastlake Ave. E., Seattle, WA 98102.

‡‡ These authors contributed equally to this work.

[1] The abbreviations used are: PITP, phosphatidylinositol transfer protein; PtdIns, phosphatidylinositol; PtdCho, phosphatidylcholine; rdgB, retinol degeneration B protein; PtdGro, phosphatidylglycerol; MAD, multiwavelength anomalous diffraction; PtdEtn, phosphatidylethanolamine; PtdOH, phosphatidic acid; START, StAR-related lipid-transfer; StAR, steroidogenic acute regulatory; PCTP, phosphatidylcholine transfer protein.

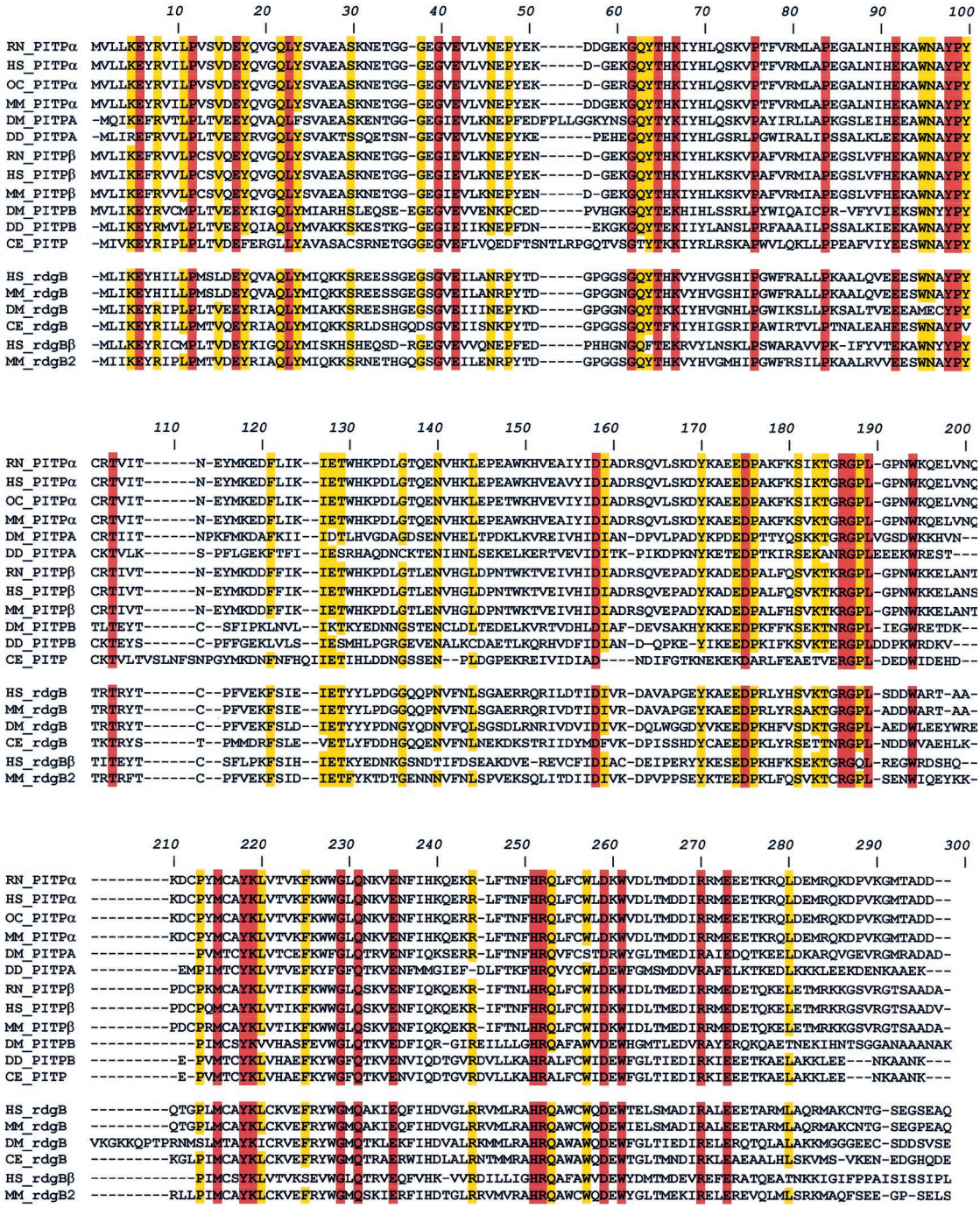

FIG. 1. **Sequence alignment of the PITP and rdgB proteins.** Amino acids showing absolute conservation among all PITP and rdgB proteins are highlighted in *red*. Amino acids exhibiting 80–99% conserved identities are highlighted in *yellow*. Species nomenclature is as follows: *RN*, *Rattus norvegicus*; *HS*, *H. sapien*; *OC*, *Oryctolagus cuniculus*; *MM*, *Mus musculus*; *DM*, *Drosophilia melanogaster*; *DD*, *D. discoideum*; *CE*, *C. elegans*.

tagged proteins, particularly at the C-terminus. To improve the likelihood that a bound phospholipid would be observed in the x-ray data, no detergents of any kind were employed in any step of purification or crystallization. Cells of *Escherichia coli* B834(DE3), a methionine auxotroph containing plasmids for expression of groELS and rat PITPα (21), were grown in chemically defined media at 20 °C with selenomethionine in place of methionine (22). The selenomethionyl-substituted protein was purified by established procedures for the wild-type protein and the bound bacterial phosphatidylglycerol (PtdGro) was replaced with *sn*-1,2-dioleoyl-PtdCho (21). The protein was crystallized under similar conditions as the wild-type protein when supplemented with seeding (23).

Structure Determination and Analysis—For x-ray data collection, crystals were mounted from the crystallization drop in a fiber loop and frozen directly in a cold nitrogen stream using an ADSC cryostat. Frozen crystals were sent to NSLS beamline X12C for "Fed-Ex Data Collection" on a Brandeis B4 CCD detector. The crystal structure of the PITPα·PtdCho complex was solved by multiwavelength anomalous diffraction (MAD) methods (24). A three-wavelength MAD x-ray data set was collected, with one wavelength at the selenium absorption edge, one at the absorption peak, and one at a low energy remote (Table I). Five of the eight selenium sites were identified by SOLVE (25) and refined by SHARP (26). The resulting electron density map was modified by solvent flipping as implemented in SOLOMON (27). From the resulting electron density map, the dominant secondary structure elements were traced. The final model was built through several cycles of manual model building with O (28), followed by refinement with CNS (29). The program DALI (30) was used to determine structurally related proteins. The lipid cavity was defined and volumes calculated using the CAST (31) web-server.

TABLE I
X-ray data collection and refinement statistics

Data collection							
Space group, Unit cell				$P2_1$ a = 43.914 Å, b = 73.773 Å, c = 48.185 Å, β = 114.732°			
Beamline				NSLS, X12-C			
Resolution				2.2 Å			
Data set	Wavelength	No. observations	No. unique reflections	Completeness[a]	I/σ	Mosaicity	R_{sym}[b]
	Å			*%*		*degree*	*%*
Peak	0.9791	41,314	13,081	90.1 (67.2)	20.2 (7.2)	0.641	4.5 (8.1)
Edge	0.9794	39,671	12,879	87.4 (60.8)	18.0 (6.2)	0.640	5.1 (9.3)
Remote	0.9500	37,690	12,669	87.8 (64.0)	18.4 (6.4)	0.624	4.6 (8.6)

Refinement	
Resolution range (Å)	50.0–2.2
R_{cryst} (%)[c]	21.2
R_{free} (%)	25.3
Number of reflections[d]	
Working set	11,516 (80.8%)
Test set	629 (4.4%)
Number of atoms	
Protein (residues 2–270)	2,228
Lipid (1 molecule PtdCho)	54
Water	55
B values (Å^2)	
Protein main-chain	17.93
Protein side-chain	21.57
Lipid	35.46
Water	16.29
rms deviations from ideality	
Bond length (Å)	0.00826
Bond angle (°)	1.2797
Ramachandran plot[e]	
Favored (%)	88.0
Allowed (%)	11.2
Generously allowed (%)	0.4
Disallowed (%)	0.4

[a] Values in parentheses indicate the highest resolution shell.
[b] $R_{sym} = \Sigma|I(hkl) - \langle I(hkl)\rangle|/\Sigma I(hkl)$.
[c] $R_{cryst} = \Sigma||F_{obs}(hkl)| - |F_{calc}(hkl)||/\Sigma|F_{obs}(hkl)|$.
[d] All data included in calculations of Working set and Test set.
[e] Glycines and prolines excluded from calculations.

RESULTS

The protein features a large concave β-sheet and several long α-helices (Fig. 2). The eight-stranded β-sheet, strands 1 to 8, has a connectivity of 71865432. The β-sheet is antiparallel, except for the orientation of strands 1 and 7, which are parallel. There are three long α-helices, composed of 5 to 7 turns (A, F, and G), and four shorter α-helices, each with less than two complete turns (B, C, D, and E). Helices A and F are oriented on the interior side of the β-sheet, with helix A aligned coincident with strand 2 and helix F oriented diagonally across the β-sheet. The phospholipid is clearly visible in the electron density map (Fig. 3), with the binding site between the interior side of the β-sheet and α-helices A and F.

Several regions of the electron density map were difficult to model. These areas consisted of residues 239–242 connecting helix F to G (containing one of the undetected selenium sites at Met^{241}) and residues 263–271 at the C terminus. The solvent-exposed side chain density of residues on helix G is somewhat weak, although the interior, buried sidechain density is unambiguous. The solvent-exposed Met^{247} has very weak side chain density and is one of the undetected selenium sites from the MAD data. The last undetected selenium site is residue 1, for which no electron density is observed.

Three Functional Regions of PITP—We designate the dominant region of the PITP structure as the lipid-binding core. This region, a cavity in which the phospholipid molecule binds, is formed by α-helices A and F and the β-sheet. Limited segments of helices A and F and strands 4 and 5 are amphipathic and provide excellent hydrophobic interaction with the phospolipid molecule (Fig. 4). The lipid-binding core comprises residues 1–118 and 191–232. Examination of the PITP structure reveals that the intervening residues 119–190 form an exten-

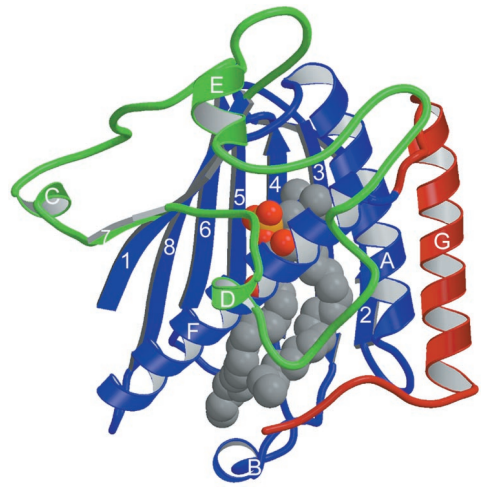

FIG. 2. **A ribbon diagram of the folding topology of PITPα·PtdCho.** The lipid-binding core of the protein is indicated in *blue*, the regulatory loop in *green*, and the C-terminal region in *red*. The phospholipid is represented in *space-filled spheres* using CPK coloring. β-sheets are labeled 1–8 and α-helices A-G. The figure was generated with MOLSCRIPT (54) and RASTER3D (55).

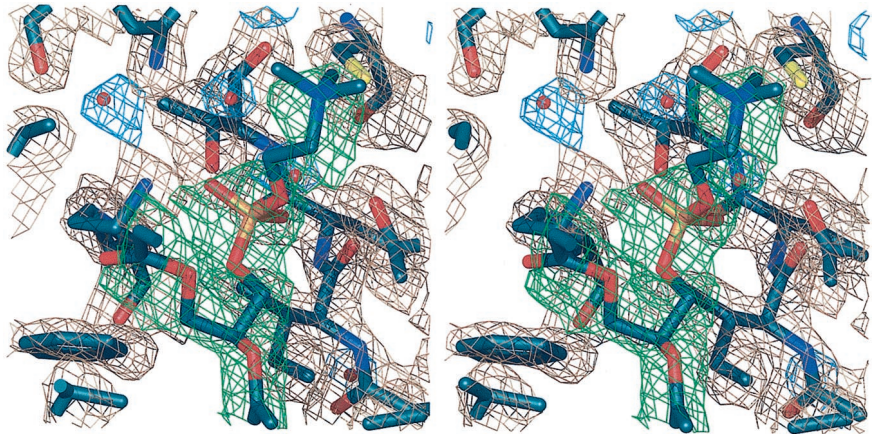

FIG. 3. **A stereo diagram of the electron density map in the vicinity of the choline group in the lipid-binding core.** An omit map was calculated in which all phospholipid and water atoms were removed and one cycle of simulated annealing was run prior to the 2Fo-Fc electron density calculation. Electron density surrounding the PtdCho molecule is *green*, around the water molecules is *light blue*, and around the protein amino acids is *brown*. All maps are contoured at 1.0 σ. Protein atoms are represented as *thick sticks* using CPK coloring and water molecules are represented by small *red spheres*.

sive loop region between strands 7 and 8. Postulating that this loop is likely required for the association of PITP with a wide variety of lipid- and protein-modifying enzymes, we refer to this region as the regulatory loop. The recent identification of Ser^{166} as a site for limited protein kinase C-dependent phosphorylation (32) supports this hypothesis. All PITPs and rdgBs studied to date contain a regulatory loop region; only *Caenorhabditis elegans* PITP lacks the equivalent Ser^{166} phosphorylation site. The remaining residues in the structure comprise the C-terminal residues 233–271. Consisting of the long α-helix G as the principal secondary structural element and an additional 11 residues that limit access to the lipid-binding cavity, we call this region the C-terminal region and suggest its critical participation in membrane association and dissociation. The C-terminal region is the least conserved region among the cytosolic PITPs and is replaced in the rdgB proteins by up to 1000 additional amino acids, some of which appear to be transmembrane.

Our functional region designation correlates reasonably well to the location of conserved amino acid residues in the PITP family (Fig. 1). The majority (nearly 75%) of the absolutely conserved amino acids are located in the lipid-binding core. Most of the others are part of the regulatory loop. Consistent with their proposed functions, both the regulatory loop and the C-terminal region were predicted to exhibit significant polypeptide backbone flexibility (33), a structural feature corroborated by specific *B* factors from the x-ray data.

Characterization of the Lipid-binding Cavity—The residues in close proximity to the PtdCho head group are shown in Figs. 3 and 4. The majority of these interacting residues are highly conserved in all PITP and rdgB proteins. Nine water molecules are within 3.2 Å of the phospholipid or an amino acid residue lining the phospholipid cavity. The phosphate oxygen O1P forms hydrogen bonds with the NZ atom of the conserved Lys^{195} and a water molecule, and oxygen O_2P hydrogen bonds with the OG1 atom of the conserved Thr^{97} and another water molecule. The solvent-accessible volume of the phospholipid-binding cavity (calculated with a 1.4 Å probe) is 670 $Å^3$, whereas the molecular-surface volume is 2725 $Å^3$. The van der Waals volume of the PtdCho molecule is 671 $Å^3$. Of the 271 residues in the protein, 72 residues (27%) have atoms contributing to the lipid cavity.

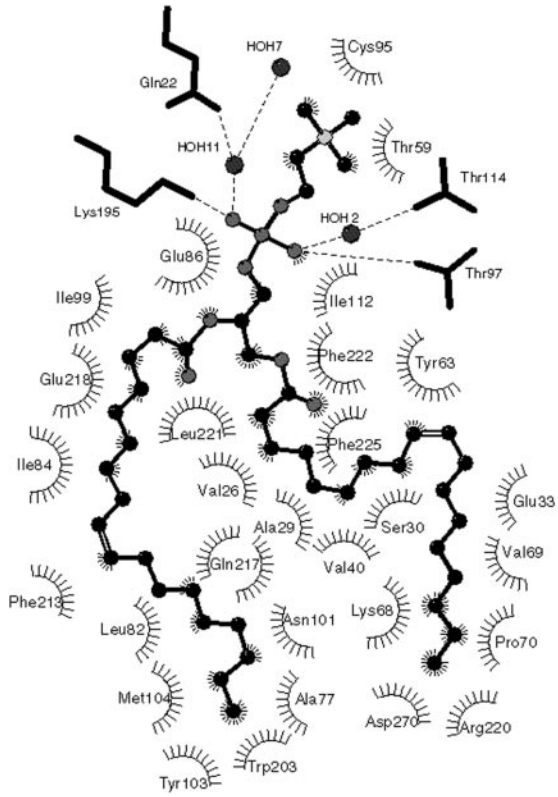

FIG. 4. **The phospholipid-binding pocket.** Residues and water molecules within 3.9 Å of the PtdCho ligand are indicated. Hydrogen bonds with the polar head group are indicated by *dashed lines*. Water molecules are indicated by *small spheres*. The *sn*-1 acyl chain is on the *right*, and the *sn*-2 acyl chain is on the *left*. The figure was generated with LIGPLOT (56).

DISCUSSION

Characteristics of the interactions between PITP and the hydrophobic region of PtdIns and PtdCho molecules have been described (34–35). Using lipids with defined fatty acyl species at their *sn*-1 and *sn*-2 positions, combined with one or more fluorescent acyl derivatives (pyrenylacyl, parinaroyl), both binding to PITP and protein-catalyzed transfer from a vesicle surface were measured. For the *sn*-1 group a broad range of structures could be accommodated, with preference for 14- and 16-carbon saturated or monounsaturated fatty acids; nevertheless, 18-carbon polyunsaturated fatty acids were still bound and transferred. In contrast, the *sn*-2 group exhibits a more restricted range, preferring 16- and 18-carbon mono- and polyunsaturated fatty acids whose double bonds were toward the

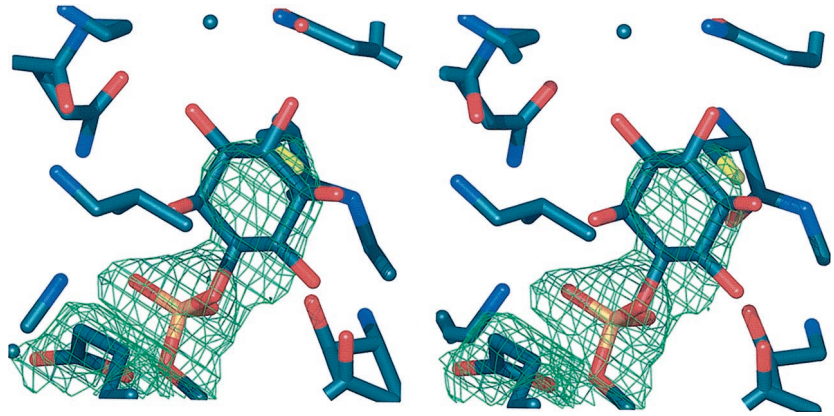

FIG. 5. **PtdIns modeled into the electron density map of PITPα·PtdCho.** Only electron density from the final 2Fo-Fc map surrounding the PtdCho is shown.

methyl-end of the lipids. PtdCho molecules containing arachidonate (20:4n-6) or docosahexaenoate (22:6n-3) in the *sn*-2 position bind weakly to PITP. It was suggested that the *sn*-2 binding site in PITP was "bottle-shaped," with the neck toward the ester linkage. Little difference was observed for acyl chain preferences between the PtdIns and PtdCho class of phospholipids.

In the PITP structure reported here, the PtdCho ligand contains two oleate (18:1n−9) acyl groups. The conformation of the *sn*-2 acyl chain is more extended than the *sn*-1 chain, such that the *sn*-2 group extends almost to the surface of the protein. The lipid cavity follows the contour of the *sn*-2 acyl chain closely, but the cavity around the *sn*-1 chain is less confining. These features may explain the poor binding of phospholipid molecules with *sn*-2 acyl moieties longer than 18 carbons and the less restrictive range of groups accommodated in the *sn*-1 acyl region of the cavity.

PITP preferentially binds PtdIns and PtdCho. Whereas PtdCho was used in the experimental protocol, inositol can be readily modeled into the electron density for the choline moiety (except for the sugar hydroxyls). There are numerous charged or polar amino acid residues in the region that may be potential hydrogen bonding partners to the inositol hydroxyls (Fig. 5). Nevertheless, the tertiary structure of the model does not completely explain polar head group specificity of PITP, for which further studies are needed.

Conformation, Stability, and Function of the C-terminal Region—To transfer a phospholipid, PITP must first bind to the membrane, exchange its bound lipid for a membrane lipid, and then dissociate from the membrane. Previous studies have shown that there are significant conformational changes in the C-terminal residues when PITP binds to lipid membranes (21). Although cytosolic PITP is highly resistant to trypsin digestion, protein bound to membranes is rapidly cleaved at Arg^{253} and Arg^{259}. In the crystal structure these two sites are part of helix G in the C-terminal region. Studies have shown that generally sites that are subject to limited proteolytic cleavage by trypsin assume a loop-like structure with a conformation similar to that of trypsin inhibitors (36). Thus, this helix must "melt" prior to cleavage by trypsin, a process facilitated by interaction with a membrane surface. The relative instability of portions of this helix is supported by the high *B* factors calculated for residues 243–250.

Residues 260–271 also appear to be important for maintaining a tight compact structure. PITPs truncated at residues 253 or 259 have more relaxed conformations than full-length PITP, defined by increased quenching of Trp fluorescence by acrylamide, increased Tyr exposure, increased reactivity of Cys, and increased anilino-naphthalene sulfonate binding (37). Inspection of the native structure shows that such changes cannot be caused by removal and exposure of residues without a conformational change in the remainder of the protein. Several studies have shown that removal of one or a few amino acids from the N- or C-terminus of a protein may have a significant effect on protein stability and/or dynamics without producing major changes in conformation (38–39). Our data on the conformation and biological activity of truncated PITPs are consistent with a critical role of the C-terminus in the complete packing of the hydrophobic core and folding and stabilization of the native structure.

The ability of PITP to bind phospholipid substrates is necessary but not sufficient for subsequent phospholipid transfer. Removal of up to 20 C-terminal residues greatly reduces phospholipid transfer, yet these truncated proteins produced in *E. coli* contain PtdGro, or less commonly, phosphatidylethanolamine (PtdEtn) with a near normal 1:1 stoichiometry (37, 40). Hence, residues 254–271 are dispensable for lipid binding, although they are important in conferring selectivity for PtdIns and for efficient transfer of phospholipids. It is not immediately obvious from the PITP structure why phospholipids such as PtdEtn and phosphatidic acid (PtdOH) are bound and/or transferred so poorly.

We had earlier reported that residues 260–271 could be eliminated with variable effects on transfer activity that reflected the composition of the membranes employed in the assay system (41). With membranes containing only PtdCho, the truncated PITP (1–259) has transfer activity identical to the full-length protein. However, with as little as 2% PtdOH in the donor and/or acceptor membranes, transfer activity decreases to 0–20% relative to that observed with PtdCho membranes. Such concentrations have minimal effect on transfer by native PITP. We demonstrated that this and the more extensively truncated PITP (1–253) have greatly enhanced affinities for membrane binding, which would result in inefficient lipid transfer activity. We suggest that the C-terminal region of PITP acts to maintain a low affinity of the full-length protein for membranes, especially those containing acidic phospholipids. Structural perturbations within the C-terminal region lead to enhanced electrostatic interactions and increased membrane affinity (41).

Structure-Function Correlation of Point Mutations—Knowledge of the tertiary structure of PITP provides an opportunity to evaluate studies describing and characterizing the random mutagenesis of the cDNA encoding rat PITPα (42). Mutations of amino acids Ser^{25}, Thr^{59}, Pro^{78}, and Glu^{248} were, in general, observed to abolish PtdIns transfer, whereas PtdCho transfer was not affected. With the exception of Ser^{25}, all are absolutely conserved among PITPs and rdgBs. Our data support a role of the Thr^{59} hydroxyl group in a putative hydrogen bonding interaction with the inositol moiety (Fig. 5) and place Ser^{25} in the vicinity of the fatty acid-glycerol ester linkages. Glu^{248} makes a salt bridge with the conserved Lys^{61} in a region close to the

choline and inositol polar head group moieties. Pro^{78} is near the end of the portion of the cavity that accommodates the *sn*-2 acyl chain. Why mutations of these residues impact selectively and variably on PtdIns binding and transfer remains unresolved.

Mutations to Glu^{6} and Pro^{12}, two absolutely conserved residues, yield poor expression of recombinant mammalian PITP in a yeast host (42). Based on our structure, these residues likely stabilize the association between the lipid-binding core and the regulatory loop. Glu^{6} participates in salt bridges with the conserved Arg^{8} and with His^{127}; similarly, Pro^{12} packs tightly against the conserved Leu^{174}.

Membrane Binding and Mechanism of Phospholipid Transfer—Analysis of the exterior features of PITP, such as charge distribution and hydrophobicity, provided little insight into what region might constitute the membrane-binding surface. We presently favor a model in which the C-terminal region is a part of this surface. In the interaction between protein and membrane, most if not all of the C-terminal region must be displaced from helix A in the lipid-binding core and acquire increased backbone flexibility sufficient to melt a portion of helix G and become sensitive to proteolytic digestion. We further envision that the refolding and reassociation of the C-terminal region with the bulk protein provides a driving force for eventual dissociation of PITP from the membrane surface.

The detailed mechanism by which PITP releases its bound lipid, exchanges it for another present in the membrane surface and dissociates from the membrane remains to be elucidated. A plausible model is one in which the C-terminal region of the protein binds to the membrane and the lipid-binding core opens, somewhat like a clam shell, exposing its bound lipid to the membrane surface. The protein-bound lipid is absorbed into the membrane and replaced by a membrane lipid. Subsequently, the C-terminal region refolds and reassociates with the body of the protein, *i.e.* the clam shell closes, and the protein dissociates from the membrane surface. The affinity for the membrane surface and the affinity for a specific phospholipid must not be too great, otherwise dissociation and transfer would be too slow and inefficient. As suggested above, the decreased rate of membrane dissociation, at least in part, makes C-terminal-truncated PITP derivatives weak catalysts of lipid exchange with membranes containing acidic phospholipids.

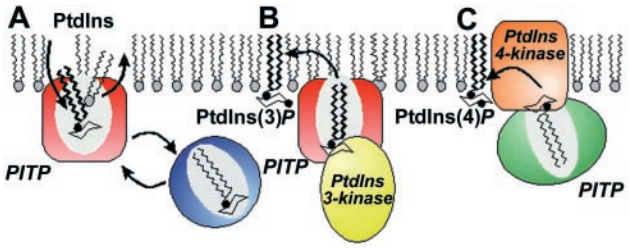

FIG. 6. **Schematic of interaction of PITP with membrane surfaces and other proteins.** *A,* protein-catalyzed phospholipid exchange and transport between membranes. *B,* interaction of a membrane-bound PITP and cytosolic PtdIns 3-kinase. *C,* interaction of PITP with a membrane-bound PtdIns 4-kinase.

To account for other biological activities of PITP, we suggest that the protein-bound phospholipid becomes accessible to phosphorylation following interaction of a lipid kinase with a complementary site on PITP, perhaps on the regulatory loop. One-third of the residues within this 72-amino acid segment are identical or >90% conserved among all PITP and rdgB proteins (Fig. 1). Protein-protein interactions are proposed to alter the conformation of PITP at the head group region of the lipid-binding core (Fig. 6). This could lead to either the presentation of PtdIns to the active site of a membrane-bound PtdIns 4-kinase or the exposure of the inositol moiety of a PITP-bound PtdIns to the action of a soluble PtdIns 3-kinase or 4-kinase (43–44). Evidence supporting such a function of PITP in substrate presentation to a PtdIns 3-kinase has been reported (10). Following modification of the inositol 3- or 4-hydroxyl function, the affinity of the product for PITP would likely decrease so significantly that it would remain with the kinase or return to the lipid surface. Consistent with this mechanism is the inability of PITP to bind and transfer PtdIns (4)P (45).

Comparison with other Lipid-binding Proteins—Using the DALI algorithm (30) to search for proteins structurally similar to PITP, the recently described START (StAR-related lipid-transfer) domain (46) was identified as sharing significant tertiary structure. MLN64 (PDB:1EM2), a protein associated with some human breast carcinomas, has served as a prototype for structure determination and mechanistic studies of the START domain (47). The MLN64 START domain contains a hydrophobic tunnel that extends the length of the protein with small openings on both ends. A nine-stranded antiparallel β-sheet and two α-helices form an interior hydrophobic chamber that is believed to be just large enough to accommodate a single molecule of cholesterol. Cholesterol was not included in the crystallization solutions, but docked into the finished protein model. START domain proteins are proposed to bind lipids and interact with membranes, properties also common to PITPs. Steroidogenic acute regulatory (StAR) protein, whose function is to deliver cholesterol to the inner mitochondrial membrane and cytochrome P450scc, contains a START domain near its C-terminus. Nearly the entire sequence of PtdCho transfer protein (PCTP), another cytosolic lipid transfer protein, consti-

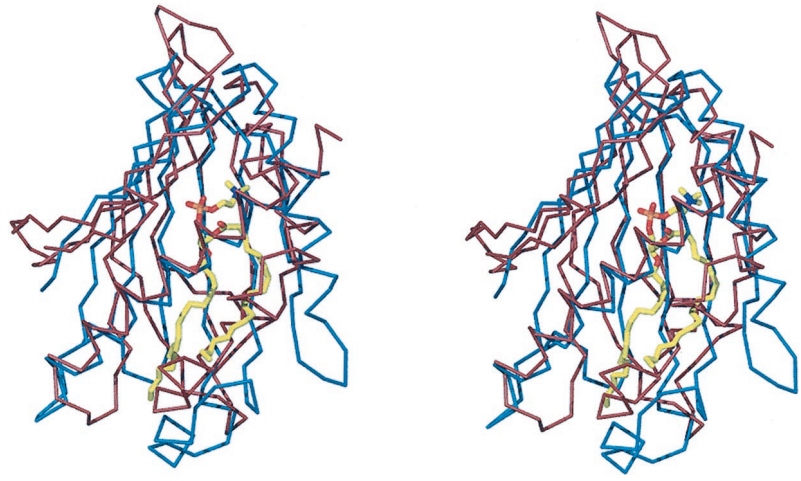

FIG. 7. **Stereo diagram of the superposition of the Cα atoms of the PITPα·PtdCho lipid-binding core and the START domain of MLN64.** The PITP trace is *blue*, and the MLN64 trace is *red*. The PtdCho molecule of PITPα·PtdCho is shown in *sticks*.

tutes a single START domain. In contrast to PITP, PCTP has a marked specificity for PtdCho and highly restricted tissue expression in mammals (2). Although not identified by the DALI search, the recently reported structure of sterol carrier protein-2 (PDB 1QND, Ref. 48) is another example of a protein with a lipid-binding core similar to that observed in MLN64 and PITP.

Despite reasonable similarity at the secondary and tertiary levels of structure (Fig. 7), there is no primary structure homology between members of the PITP family and proteins with a START domain. It should be noted that the lipid cavity in PITP is larger than the cavity in MLN64. Upon superposition, one of the α-helices comprising the putative lipid-binding cavity of MLN64 clashes with the *sn*-1 acyl chain of the bound PtdCho in the PITP structure. This is not surprising in that PITP binds diacyl phospholipids, whereas MLN64 binds the more compact cholesterol molecule. The START and PITP protein families represent an excellent example of functional evolutionary convergence to generate comparable domain architecture and related biological function from apparently unrelated genetic information.

Fungi and plants contain Sec14p, a cytosolic protein that transports PtdIns and PtdCho (13, 49–52) and is required for protein export and cell viability. Recently, the three-dimensional structure of *Saccharomyces cerevisiae* Sec14p, one member of this conserved family, was reported (53). PITP and Sec14p are similar in size, exhibit similar *in vitro* lipid-binding specificity and transport abilities and display significant and highly complementary interspecies activity. However, the two proteins have little structural similarity. In contrast to the PITPα·PtdCho structure, Sec14p structure has no bound phospholipid molecule.

Conclusions—Elucidation of the PITPα·PtdCho structure reveals a complex amphipathic lipid completely enclosed within a folded polypeptide cavity. The three functional regions of the protein provides a molecular framework for understanding the details of protein-lipid interactions on several levels. Within its lipid-binding core, PITP has been shown to sequester phospholipids from the aqueous environment. Lipid ligand specificity, whereas not completely explained by the tertiary structure, is dictated by extensive noncovalent interactions. The C-terminal region of PITP is proposed to promote the transient association to and dissociation from lipid surfaces. Through its regulatory loop, PITP is thought to present lipid substrates to kinases for subsequent phosphorylation. Further mutagenic and structural studies of PITP and other members of the PITP-rdgB family are required to test these and other hypotheses. Detailed analyses of PITP interactions with membranes and kinases are needed to gain a more meaningful understanding of the role of PITP in cellular phospholipid metabolism.

Acknowledgments—The atomic coordinates for the crystal structure of PITPα·PtdCho have been deposited in the Research Collaboratory for Structural Bioinformatics Protein Data Bank with accession code 1FVZ. We thank Chuong Doan and Sienna Sifuentes for technical assistance. Diffraction data for this study were collected at Brookhaven National Laboratory in the Biology Department single-crystal diffraction facility at beamline X12-C in the National Synchrotron Light Source. This facility is supported by the United States Department of Energy Offices of Health and Environmental Research and of Basic Energy Sciences under prime contract DE-AC02-98CH10886, by the National Science Foundation and by National Institutes of Health Grant 1P41 RR12408-01A1. We are grateful for the assistance of Michael Becker and Robert Sweet with "Fed-Ex Data Collection" at X12-C.

REFERENCES

1. Trotter, P. J., and Voelker, D. R. (1994) *Biochim. Biophys. Acta* **1213,** 241–262
2. Wirtz, K. W. A. (1997) *Biochem. J.* **324,** 353–360
3. Lev, S., Hernandez, J., Martinez, R., Chen, A., Plowman, G., and Schlessinger, J. (1999) *Mol. Cell. Biol.* **19,** 2278–2288
4. Swigert, P., Insall, R., Wilkins, A., and Cockcroft, S. (2000) *Biochem. J.* **347,** 837–843
5. The *C. elegans* sequencing consortium (1998) *Science* **282,** 2012–2018
6. Thomas, G. M. H., Cunningham, E., Fensome, A., Ball, A., Totty, N. F., Truong, O., Hsuan, J. J., and Cockcroft, S. (1993) *Cell* **74,** 919–928
7. Hay, J. C., and Martin, T. F. J. (1993) *Nature* **366,** 572–575
8. Kauffmann-Zeh, A., Thomas, G. M. H., Ball, A., Prosser, S., Cunningham, E., Cockcroft, S., and Hsuan, J. J. (1995) *Science* **268,** 1188–1190
9. Cunningham, E., Tan, S. K., Swigert, P., Hsuan, J., Bankaitis, V., and Cockcroft, S. (1996) *Proc. Natl. Acad. Sci. U. S. A.* **93,** 6589–6593
10. Panaretou, C., Domin, J., Cockcroft, S., and Waterman, M. D. (1997) *J. Biol. Chem.* **272,** 2477–2485
11. Ohashi, M. de Vries, K. J., Frank, R., Snoek, G., Bankaitis, V., Wirtz, K., and Huttner, W. B. (1995) *Nature* **377,** 544–547
12. Paul, K. S., Bogan, A. A., and Waters, M. G. (1998) *FEBS Lett.* **431,** 91–96
13. Cockcroft, S. (1998) *BioEssays* **20,** 423–432
14. Martin, T. F. J. (1997) *Curr. Opin. Neurobiol.* **7,** 331–338
15. Tanaka, S., and Hosaka, K. (1994) *J. Biochem.* (*Tokyo*) **115,** 981–984
16. Dickeson, S. K., Lim, C. N., Schuyler, G. T., Dalton, T. P., Helmkamp, G. M., Jr., and Yarbrough, L. R. (1989) *J. Biol. Chem.* **264,** 16557–16564
17. Vihtelic, T. S., Goebl, M., Milligan, S., O'Tousa, J. E., and Hyde, D. R. (1993) *J. Cell Biol.* **122,** 1013–1022
18. Guo, J., and Yu, F. X. (1997) *Dev. Genet.* **20,** 235–245
19. Chang, J. T., Milligan, S., Li, Y., Chew, C. E., Wiggs, J., Copeland, N. G., Jenkins, N. A., Campochiaro, P. A., Hyde, D. R., and Zack, D. J. (1997) *J. Neurosci.* **17,** 5881–5890
20. Aikawa, Y., Hara, H., and Watanabe, T. (1997) *Biochem. Biophys. Res. Comm.* **236,** 559–565
21. Tremblay, J. M., Helmkamp, G. M., Jr., and Yarbrough, L. R. (1996) *J. Biol. Chem.* **271,** 21075–21080
22. Neidhardt, F. C., Bloch, P. L., and Smith, D. F. (1975) *J. Bacteriol.* **119,** 736–747
23. Oliver, R. L., Tremblay, J. M., Helmkamp, G. M., Jr., Yarbrough, L. R., Breakfield, N. W., and Yoder, M. D. (1999) *Acta Crystallogr. Sect. D* **55,** 522–524
24. Hendrickson, W. A. (1991) *Science* **254,** 51–58
25. Terwilliger, T. C., and Berendzen, J. (1999) *Acta Crystallogr. Sect. D* **55,** 849–861
26. La Fortelle, E., and Bricogne, G. (1997) *Methods Enzymol.* **276,** 472–494
27. Abrahams, J. P., and Leslie, A. G. W. (1996) *Acta Crystallogr. Sect. D* **52,** 32–42
28. Jones, T. A., Cowan, S., Zou, J.-Y., and Kjeldgaard, M. (1991) *Acta Crystallogr. Sect. A* **47,** 110–119
29. Brünger, A. T., Adams, P. D., Clore, G. M., DeLano, W. L., Gros, P., Grosse-Kunstleve, R. W., Jiang, J.-S., Kuszewski, J., Nilges, N., Pannu, N. S., Read, R. J., Rice, L. M., Simonson, T., and Warren, G. L. (1998) *Acta Crystallogr. Sect. D* **54**, 905–921
30. Holm, L., and Sander, C. (1993) *J. Mol. Biol.* **233,** 123–138
31. Liang, J., Edelsbrunner, H., and Woodward, C. (1998) *Prot. Sci.* **7,** 1884–1897
32. van Tiel, C. M., Westerman, J., Paasman, M., Wirtz, K. W. A., and Snoek, G. T. (2000) *J. Biol. Chem.* **275,** 21532–21538
33. Karplus, P. A., and Schultz, G. E. (1985) *Naturwissenschaften* **72,** 212–213
34. van Paridon, P. A., Gadella, T. W. J., Jr., Somerharju, P. J., and Wirtz, K. W. A. (1988) *Biochemistry* **27,** 6208–6214
35. Kasurinen, J., van Paridon, P. A., Wirtz, K. W. A., and Somerharju, P. (1990) *Biochemistry* **29,** 8548–8554
36. Hubbard, S. J., Eisenmenger, F., and Thornton, J. M. (1994) *Prot. Sci.* **3,** 757–768
37. Voziyan, P. A., Tremblay, J. M., Yarbrough, L. R., and Helmkamp, G. M., Jr.,. (1996) *Biochemistry* **35,** 12526–12531
38. Trevino, R. J., Gliubich, F., Berni, R., Cianci, M., Chirgwin, J. M., Zanotti, G., and Horowitz, P. M. (1999) *J. Biol. Chem.* **274,** 13938–13947
39. de Prat Gay, G., Ruiz-Sanz, J., Neira, J. L., Corrales, F. J., Otzen, D. E., Ladurner, A. G., and Fersht, A. R. (1995) *J. Mol. Biol.* **254,** 968–979
40. Hara, S., Swigart, P., Jones, D., and Cockcroft, S. (1997) *J. Biol. Chem.* **272,** 14908–14913
41. Tremblay, J. M., Voziyan, P. A., Helmkamp, G. M., Jr., and Yarbrough, L. R. (1998) *Biochim. Biophys. Acta* **1389,** 91–100
42. Alb, J. G., Jr., Gedvilaite, A., Cartee, R. T., Skinner, H. B., and Bankaitis, V. A. (1995) *Proc. Natl. Acad. Sci. U. S. A.* **92,** 8826–8830
43. Balla, T. (1998) *Biochim. Biophys. Acta* **1436,** 69–85
44. Wymann, M. P., and Pirola, L. (1998) *Biochim. Biophys. Acta* **1436,** 127–150
45. Schermoly, M. J., and Helmkamp, G. M., Jr.,. (1983) *Brain Res.* **268,** 197–200
46. Ponting, C. P., and Aravind, L. (1999) *Trends Biochem. Sci.* **24,** 130–132
47. Tsujishita, Y., and Hurley, J. H. (2000) *Nat. Struct. Biol.* **7,** 408–414
48. Garcia, F. L., Szyperski, T., Dyer, J. H., Choinowski, T., Seedorf, U., Hauser, H., and Wüthrich, K. (2000) *J. Mol. Biol.* **295,** 595–603
49. Kearns, B. G., Alb, J. G., Jr., and Bankaitis, V. A. (1998) *Trends Cell Biol.* **8,** 276–282
50. Bankaitis, V. A., Aitken, J. R., Cleves, A. E., and Dowhan, W. (1990) *Nature* **347,** 561–562
51. Daum, G., and Paltauf, F. (1984) *Biochim. Biophys. Acta* **794,** 385–391
52. Jouannic, N. Lepetit, M., Vergnolle, C., Cantrel, C., Gardies, A.-M., Kader, J.-C., and Arondel, V. (1998) *Eur. J. Biochem.* **258,** 402–410
53. Sha, B., Phillips, S. E., Bankaitis, V. A., and Luo, M. (1998) *Nature* **391,** 506–510
54. Kraulis, P. J. (1991) *J. App. Crystallogr.* **24,** 946–950
55. Merritt, E. A., and Murphy, M. E. P. (1994) *Acta Crystallogr. Sect. D* **50,** 869–873
56. Wallace, A. C., Laskowski, R. A., and Thornton, J. M. (1995) *Prot. Eng.* **8,** 127–134